



## A modeling approach for cell growth based on enzyme kinetics

Stanko Dimitrov

University of Sofia, Faculty of Mathematics and Informatics,  
email: [stankod@fmi.uni-sofia.bg](mailto:stankod@fmi.uni-sofia.bg)

### Abstract

The enzyme kinetics reaction scheme of single enzyme-substrate dynamics, originally proposed by V. Henri, is considered. The system of ODEs induced by the reaction scheme is compared to two approximate models, namely the Michaelis-Menten model and the model of exponential decay. Validity conditions for the Michaelis-Menten model are briefly reviewed. A case specific for “superefficient enzymes” is used as a setting for a comparison between the three models via computational experiments. The case study proves the importance of validating the applicability of the approximate model.

A novel cell growth model is proposed and analyzed. The approach of model development is to make use of the original Henri enzyme kinetics law in the context of metabolic processes in living cells, namely cell growth. Two approximations corresponding to different cell growth phases are introduced in order to study the model analytically.

---

The presented work is a University of Sofia student Master Thesis.

---

**Citation:** Stanko Dimitrov, A modeling approach for cell growth based on enzyme kinetics, <http://dx.doi.org/10.11145/bmc.2016.12.297>

*Keywords: enzyme kinetics, cell growth, reaction equations, Michaelis constant, biomass-substrate-product dynamics*

## 1 Introduction

Since its discovery around 1900, the Henri enzyme kinetics law has been intensively applied in many fields of life sciences. Two types (or stages) of its application can be distinguished: a first type of applications in biotechnological (fermentation) processes where the enzymes are often produced by bacterial cells, and a second type of applications in metabolic processes in living cells.

The first type of applications are often denoted as *in vitro* whereas the second one—*in vivo*. During *in vitro* processes one is usually interested in the transformation of as much as possible quantity of substrate into product using thereby as little as possible quantity of enzymes. Thus, the ratio enzyme/substrate *in vitro* is usually very small, whereas *in vivo* this may not be the case. For the *in vitro* case the approximate Michaelis-Menten model has been proposed together with a simple protocol for the calculation of the two parameters involved in the model ( $V_{max}$  and  $K_m$ ).

The Michaelis-Menten model has proved to be extremely useful and has become very popular amongst biological scientists. Plausible biochemical mechanisms (known as Briggs-Haldane interpretations) have been found also known as (standard) quasi-steady-state approximation (sQSSA) criteria for the validity of the Michaelis-Menten model.

With the necessity of considering *in vivo* processes, three approaches can be possibly followed. One is to extend the applicability (validity) of the Michaelis-Menten model by finding more general criteria than the standard enzyme/substrate ratio criterion (the sQSSA condition), such as the so-called rQSSA and the tQSSA criteria. A disadvantage of this approach is that these criteria are more complex to check and involve the computation of new parameters, thereby still producing often very rough results.

Another approach could be to make use of other approximate phe-

nomenological models together with corresponding validity criteria, such as the first order decay model. As demonstrated in Section 3.1 in certain situations the decay model can give a better approximation than the Michaelis-Menten model.

A third approach would be to make use of the original (exact) Henri enzyme kinetics law and the induced system of ODEs. The proponents of the approximate models underline that the Henri law induced system of ODEs is too complex to use in real applications and cumbersome to handle. This could be overcome to a certain extent with the use of powerful contemporary mathematical and computational tools to make the exact Henri model easily applicable in practice. In particular, familiar computer algebra systems (CAS) such as *Mathematica* and *MATLAB* can be used to handle the ODE system induced by the Henri law in order to conduct numerical experiments. To efficiently apply the original Henri law, it is necessary to compute the three Henri's rate constants from time-course kinetic measurements using computer simulations. However, such time-course measurement data are usually not explicitly available in the literature. In the best case some graphs are published together with the computed Michaelis constant  $K_m$  which is of little use for the computation of the three Henri rate constants.

We pose a case for the use of the aforementioned third approach in the modeling of metabolic processes in living cells. Namely, the original Henri enzyme kinetics law is used as a foundation for the development of a cell growth model. The proposed model is studied analytically and computationally in Section 4.

The proposed cell growth model is further supported by evidence of the advantages in use of exact, mechanistic models such as the HMM model (Section 3).

**Section 2** contains a review of the original Henri-Michaelis-Menten reaction scheme (briefly denoted as HMM-scheme) and the approximate Michaelis-Menten model (MM-model). The HMM reaction scheme induces (via the mass action law) a system of ordinary differential equations (denoted HMM-system) while the approximate MM-model

is derived from the HMM-system using well known assumptions ([3], [4], [5], [6], [16], [18], [21], [22], [28]). The criteria for the validity of the MM-model is briefly commented on.

**Section 3** is devoted to computational experiments that reveal some details on the conditions under which the approximate Michaelis-Menten model is adequate. The analysis is based on a well-defined criterion for the validity of the model, as well as general analysis of its dynamics based on the ODE system. Cases where the biomass solutions of the two models are close, but the suggested dynamics differ significantly, are also presented.

The obtained results support the use of reaction schemes, such as the one proposed by V. Henri in the development of dynamical models. Furthermore, the analysis of these models provides opportunities for better understanding of the underlying physical processes.

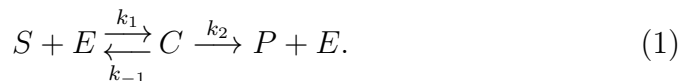
**Section 4** is devoted to the analytical and computational study of a novel cell growth model. The model is inspired by the use of the original HMM reaction scheme in the field of enzyme kinetics. Similarities in approaches of modeling enzyme kinetics processes and cell growth dynamics are taken into consideration in the development of the model. Further analysis shows the applicability of such approaches, as well as the invaluable insight into the dynamics and mechanics of the underlying physical processes they provide.

The computational experiments and case studies on enzyme kinetics, that supported and shaped the development of the novel model (Section 4), have been part of previous research [9], [10]. Section 2 and Section 3 are based on the work from reference [10]. Section 4 consists entirely of unpublished work and draws attention to the modeling of cell growth. The introduced model is studied analytically and numerically, supporting the analysis with many figures of numerical solutions, nullclines, phase portraits, etc.

## 2 Enzyme kinetics basic models

### 2.1 Henri's reaction scheme

The following reaction scheme of simple enzyme-substrate dynamics, where two fractions of the enzyme (free and bound) are involved, has been proposed by Victor Henri [8], [13]–[14]:



Henri's reaction scheme (1) describes the reaction mechanism between an enzyme  $E$  with a single active site and a substrate  $S$ , forming reversibly an enzyme-substrate complex  $C$ , which then yields irreversibly a product  $P$ . Reaction scheme (1) says that during the transition of the substrate  $S$  into product  $P$  the enzyme  $E$  bounds the substrate into a complex  $C$  having different properties than the free enzyme and thus being necessarily considered as a separate substance.

Denoting the concentrations  $s = [S]$ ,  $e = [E]$ ,  $c = [C]$ ,  $p = [P]$  and applying the mass action law to Henri's reaction scheme (1) we obtain the following system of ODEs:

$$\begin{aligned} ds/dt &= -k_1es + k_{-1}c, \\ de/dt &= -k_1es + (k_{-1} + k_2)c, \\ dc/dt &= k_1es - (k_{-1} + k_2)c, \\ dp/dt &= k_2c, \end{aligned} \quad (2)$$

to be further called the HMM-system—in tribute to V. Henri, as well to L. Michaelis and M. Menten [21]. If the three rate constants  $k_1, k_{-1}, k_2$  are known, system (2) can be treated as a Cauchy problem with initial conditions  $s(0) = s_0 > 0$ ,  $e(0) = e_0 > 0$ ,  $c(0) = 0$ ,  $p(0) = 0$ .

In practice, the HMM-system rate constants  $k_1, k_{-1}, k_2$  are often not known and have to be determined for every enzyme-substrate pair.

The contemporary approach to this task is to consider the rate constants as parameters in the dynamic HMM-system (2) and to compute them by fitting the solutions of the system to time course experimentally measured data [10].

## 2.2 Michaelis-Menten equation

Applying the quasi-steady-state assumption (QSSA) to HMM-system (2), one derives the following approximate equations for the substrate rate  $ds/dt$  and the complex  $c$  [5], [21], [22]:

$$c = \frac{e_0 s}{K_m + s}, \quad (3)$$

$$\frac{ds}{dt} = -\frac{V_{max}s}{K_m + s} = -\mu(s), \quad (4)$$

where the right-hand side function  $\mu(s) = V_{max}s/(K_m + s)$  is known as “specific growth function” in cell growth modeling [19]. The solution  $s_m$  of equation (4) is an approximation of the solution  $s$  of system (2). The QSSA is reasonably applied, e.g. when the ratio  $[E]/[S]$  is small so that fermentation continues for a considerably long time interval while the concentration  $c = [C]$  of the bound enzyme is nearly constant. This can be achieved e.g. when the condition  $e_0 \ll s_0$  holds. Let us also remind that under the validity of QSSA the complex concentration  $c = [ES]$  is expressed in terms of the MM-substrate concentration via equation (3).

In their paper, Michaelis and Menten discuss in detail Henri’s reaction scheme and equation (4) known as Michaelis-Menten equation to be further denoted as MM-model [21]. In addition, Michaelis and Menten proposed a protocol for the practical calculation of the constants  $V_{max}$  and  $K_m$  in ODE (4). The constant  $K_m$  is known as Michaelis constant [8], [27].

The MM-equation (4) can be written in the form:

$$\frac{ds}{dt} = -\frac{V_{max}s}{K_m + s} = -\frac{V_{max}}{K_m/s + 1},$$

showing that for large values of  $s$  the right-hand side is close to the constant  $-V_{max}$ , hence, the substrate uptake rate  $|ds/dt|$  is nearly equal to the constant  $V_{max}$ .

Equation (4) produces a good approximation  $s_m$  for  $s$  under certain conditions (sometimes called validity criteria) [3], [5], [11], [12], [18], [28], [24], [25]. Thus, the condition  $e_0 \ll s_0$  assures good approximation and is ubiquitous for many fermentation and biotechnological processes, but may not be present, as in living cells [1], [26].

## 2.3 Relations between the rate parameters

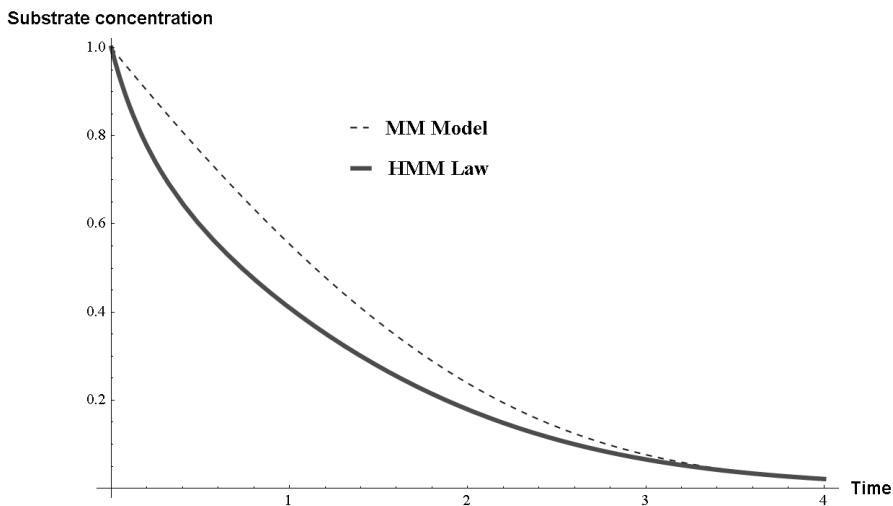


**Figure 1:** Graphics of the substrate dynamics according to the HMM-system (2) and MM-model (4). The rate constants of system (2) are  $k_1 = 2.62, k_{-1} = 0.1, k_2 = 1.25$ , initial conditions:  $s_0 = 1, e_0 = 1.5$  (the system is dimensionless); the parameters of model (4) are  $K_m = (k_{-1} + k_2)/k_1 = 0.51526, V_{max} = k_2 e_0 = 1.875$ .

In (Figure 1) the substrate uptake  $s$  is visualized in two different ways. The two graphics present the approximate solution  $s_m$  to the MM-model (4) as well as the original solution  $s$  of the HMM-system (2). In this example the kinetic parameters are chosen so that the

validity conditions of the MM-model do not hold, and the difference of the solutions for the substrate of the two systems is visible. In order to test whether the validity conditions of the approximate model do hold, the two solutions are compared.

In order to correctly compare the solutions  $s$  and  $s_m$ , one has to establish certain consistency relations between the parameters in the MM-equation and the HMM-system. From the derivation of the MM-equation, see e.g. [22], we know that the parameters in model (4) can be expressed by the parameters in system (2) by means of the relations:

$$V_{max} = k_2 e_0, \quad K_m = (k_{-1} + k_2)/k_1. \quad (5)$$

On the other hand, the three parameters in system (2) cannot be uniquely determined by the two parameters in model (4). The following computational examples show how the approximate substrate concentration solution  $s_m$  to the MM-equation may look like depending on the initial values of the substrate  $s_0$  and the enzyme  $e_0$ .

According to the MM-model we have  $ds/dt = V_{max}s/(K_m + s)$ . The two constants  $V_{max}$  and  $K_m$  can be experimentally determined following the MM-protocol. If the MM-model is valid we have  $V_{max} \approx k_2 e_0$ . Using this expression one can calculate the value  $k_{cat} = V_{max}/e_0$ . Hence  $k_{cat} \approx k_2$  if the validity conditions for the MM-model take place.

Assuming that  $k_2$  is a universal rate constant for a given specific reaction, then it should not depend on whether the validity conditions take place or not (e.g. if  $k_2$  is computed in an experiment with  $e_0 \ll s_0$ , it should be the same constant in another experiment with  $e_0 > s_0$ ).

Thus, we may assume  $k_{cat} \approx k_2$ . This gives a method for evaluating the HMM-rate constant  $k_2$ . However, it is not possible to obtain any information about the HMM-rate parameters  $k_1, k_{-1}$  on the basis of the MM-model, respectively, the MM-protocol.

# 3 Case Study of the use of the Henri-Michaelis-Menten model

## 3.1 Computational examples: model comparison

In this section, the results of several numerical studies aiming at the comparison of the substrate dynamics of the two models are presented (2), (4). The values of the dimensionless parameters  $K = K_m/s_0$  and  $\varepsilon = e_0/s_0$  play an important role in our analysis, because they can significantly influence the behavior of the system. The values of the two system characteristic parameters  $K, \varepsilon$  are varied in the numerical study, in order to present results for the cases when  $K \leq 1$  and  $\varepsilon \ll 1, \varepsilon > 1$ , as well as  $K \gg 1$  and  $\varepsilon \ll 1, \varepsilon > 1$ . The values of the HMM rate constants  $k_1, k_{-1}, k_2$  are kept the same for all cases as follows:  $k_1 = 0.1, k_{-1} = 0.01, k_2 = 10$ . The Michaelis constant consistent with these values, according to relations (5), is equal to:  $K_m = (k_{-1} + k_2)/k_1 = 100.1$ .

### 3.1.1 Criterion for good approximation

An important requirement for the validity of the MM-model (4) is the following condition:

$$\frac{k_2 e_0}{k_1 (s_0 + K_m)^2} = \left( \frac{e_0}{s_0 + K_m} \right) \left( \frac{1}{1 + (k_{-1}/k_2) + (s_0 k_1/k_2)} \right) \ll 1. \quad (6)$$

Condition (6) can be derived from the relation between the estimates of two timescales  $t_c$  and  $t_s$  ([18], [22], ch. 6.2). The timescale  $t_c$  corresponds to the faster reaction, involving the enzyme and the complex. Complex formation is the most significant process during this timescale. The longer timescale,  $t_s$ , corresponds to the product synthesis and substrate utilization. It is natural to assume  $t_c \ll t_s$ , which in turn leads to criterion (6).

The condition  $e_0 \ll s_0$  implies criterion (6), but in case when  $e_0 \ll s_0$  does not hold, the MM-model could still be a good approximation if  $K_m$  is large enough ( $K_m \gg s_0$  and also  $k_{-1} \ll k_2$ ). In order

to provide a more comprehensive explanation of this statement, we should consider the non-dimensionalized system proposed in [22], as well as the form of the MM-model under the following conditions:

$$\begin{aligned}\tau &= k_1 e_0 t, & u(\tau) &= s(t)/s_0, & v(\tau) &= c(t)/e_0, \\ \lambda &= k_2/(k_1 s_0), & K &= K_m/s_0, & \varepsilon &= e_0/s_0,\end{aligned}$$

$$du/d\tau = -u + (u + K - \lambda)v, \quad (7)$$

$$\varepsilon dv/d\tau = u - (u + K)v, \quad u(0) = 1, \quad v(0) = 0. \quad (8)$$

First, the dynamics of  $v$  can be summarized as follows:  $v$  increases from  $t = 0$  until it reaches its maximum at  $v = u/(u + K)$ , after that it decreases back to 0. An important point is that if  $K$  is large then the maximum of  $v$  will be smaller. Furthermore, larger  $K$  indicates either larger  $k_2$  and/or larger  $k_{-1}$  values in comparison to  $s_0 k_1$ . The most common ranges of the values of  $k_2$  and  $k_1$  are considered to be  $k_2 \in [10^3, 10^6]s^{-1}$ ,  $k_1 \in [10^7, 10^{10}]M^{-1}s^{-1}$  from many sources (such as [2], [29], [32]). Some authors ([29], [23]) also state that for “superefficient enzymes” (or enzymes with perfect kinetics) the rate-limiting step is the substrate-enzyme association step. Such enzymes are thought to have reached kinetic perfection or catalytic perfection [30], and that  $k_2 \gg k_{-1}$  holds for them [29]. Additionally, in certain rare cases the concentration of substrate is very small in comparison to the available enzyme [1]. Such cases may include formation of cellular micro-compartments, enzymatic activity in mammalian muscle tissue and others [1]. In these cases the concentration of substrate can even reach values  $s_0 \ll k_2/k_1$ . Assuming that the following holds for some of the cases we study: (1) the substrate concentration is sufficiently low, so that  $k_2 \gg s_0 k_1$ , (2) the formed enzyme-substrate complex breaks down to product and enzyme faster than it dissociates to substrate and enzyme, thus  $k_2 \gg k_{-1}$ . For the enzymes under consideration the rate-limiting step of their reactions is the substrate-enzyme association step and due to their catalytic perfection a small amount of complex is present during the whole process.

It should be noted that for the case studies in the following section we have used values of the kinetic parameters different than the ones derived from real experiments for convenience and simplicity. However, the conditions we rely on ( $k_2 \gg s_0 k_1$ ,  $k_2 \gg k_{-1}$ ) are kept valid when examining the case  $K \gg 1$  and we argue that parameters close to the ranges observed in real experiments exist, based on the aforementioned statements.

We could also rewrite the Michaelis-Menten model (4) under the assumptions  $K \gg 1$ ,  $k_{-1} \ll k_2$  in the following form:

$$\frac{ds}{dt} = -\frac{V_{max}s}{K_m + s} = -\frac{k_2 e_0 s}{\frac{k_{-1} + k_2}{k_1} + s} = -\frac{k_1 k_2 e_0 s}{k_{-1} + k_2 + k_1 s} \sim -k_1 e_0 s.$$

The obtained form suggests a much simpler reaction and a negligible role of the intermediate complex. Thus, the product formation is only limited by the kinetic constant  $k_1$ . Also, the derived equation is identical to the exact substrate ODE from system (2) if we assume  $e = e_0$ ,  $c \sim 0$ , which would be natural given the kinetic parameter assumptions we have made.

### 3.1.2 The exponential decay model

We may argue that under the conditions discussed above the second terms in the non-dimensionalized system (7–8) are almost 0. System (7–8) can be approximated as follows:

$$du/d\tau = -u, \quad dv/d\tau = \frac{u}{\varepsilon}; \quad u(0) = 1, \quad v(0) = 0. \quad (9)$$

The solution  $u$  of this dynamical system is identical to the solution  $s_d$  of the substrate dynamics induced by the simple reaction scheme:



wherein  $S$  is the substrate,  $E$  is the enzyme and  $P$  is the product. Reaction scheme (10) says, differently to reaction scheme (1), that during the transition of the substrate  $S$  into product  $P$  the enzyme  $E$  does

not bound the substrate into a complex. Applying the mass action law, assuming  $e = [E]$  constant, the kinetic scheme (10) leads to the following “exponential decay” differential equation for the substrate concentration  $s_d = [S]$ :

$$\frac{ds_d}{dt} = -kes_d. \quad (11)$$

Solving the Cauchy problem related to equation (11), having set  $e = e_0$ , we obtain  $k = k_1$ . Indeed, the solution of equation (11) is  $s_d(t) = s_0e^{-e_0kt}$ . If we then solve the Cauchy problem (9), we would obtain  $s(t) = s_0e^{-e_0k_1t}$  after converting it back to the initial variables.

Our analysis shows that model (11) deserves to be included in the comparison of the two models (2), (4). We shall further show that under the conditions  $K \gg 1, k_{-1} \ll k_2$  the three models (2), (4), and (11) do indeed provide almost identical results and that the substrate solution of the MM-model may provide a good approximation even though  $e_0 \ll s_0$  does not necessarily hold.

### 3.1.3 Computational examples: two cases

**Case 1.**  $K \approx 1$  ( $s_0 \approx K_m$ ) (also valid for the range  $K \leq 1$  ( $s_0 \geq K_m$ )).

**Computational example 1.1.** In this example the MM- HMM-solutions for the substrate are close when  $\varepsilon$  is small (Figure 2).

The values of the initial conditions used in the models are as follows:  $s_0 = 100, e_0 = 0.1, c_0 = 0, p_0 = 0$ . The values of the parameters in model (4) are consistent with the initial conditions and rate parameters in system (2) and are calculated using (5) as  $V_{max} = k_2e_0, K_m = (k_{-1} + k_2)/k_1$ . The parameter  $k$  in the “exponential decay” differential equation (11) is set to be equal to  $k_1$  as derived in the previous section. In all the examples that follow, only  $s_0$  and  $e_0$  will vary, all the other parameters of the model will have the same values as in this example or they will be calculated using the corresponding  $s_0, e_0$ .

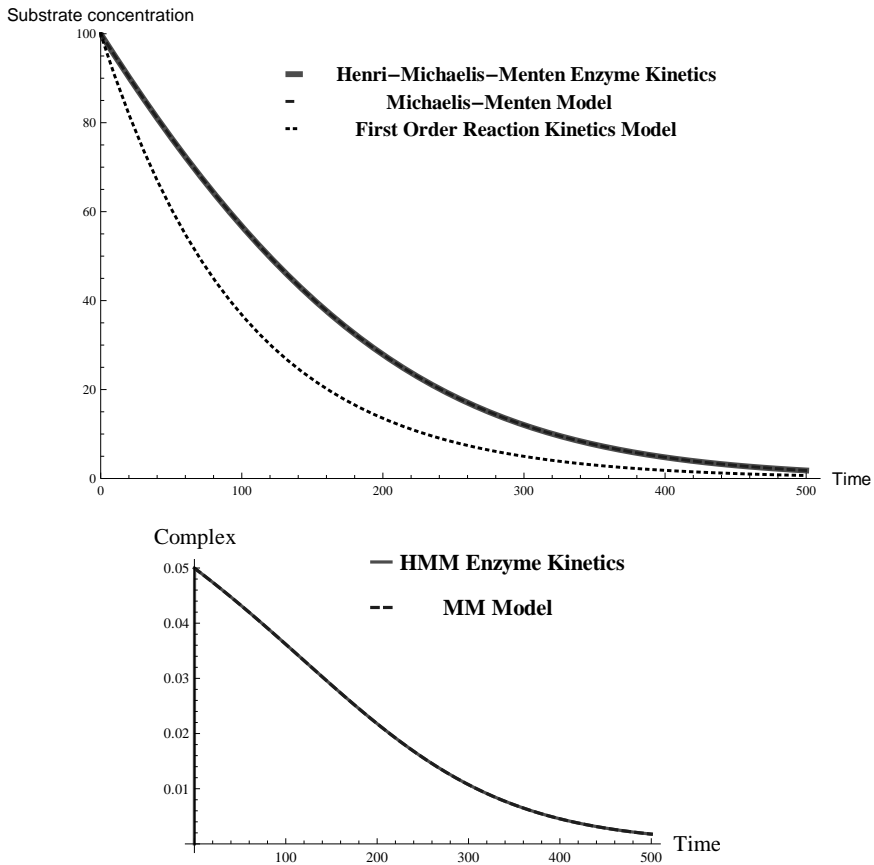


**Figure 2:** The solutions of the substrate (for models (2), (4), (11)) and the complex (for models (2), (4)) in the case  $\varepsilon = 10^{-3} \ll 1$ . Kinetic parameter values:  $k_1 = 0.1, k_{-1} = 0.01, k_2 = 10, K_m = (k_{-1} + k_2)/k_1 = 100.1, V_{max} = k_2 e_0 = 1$ ; initial conditions:  $s_0 = 100, e_0 = 0.1, c_0 = 0, p_0 = 0$ . Under these conditions the MM-model clearly serves as a good approximation of the exact HMM-system.

This numerical example demonstrates that when the condition  $\varepsilon \ll 1$  holds then the MM-model (4) can be a very good approximation of the original HMM-system (2). Note that in this example the Michaelis constant  $K_m$  used for the computation of the approximate MM-solution is derived from the HMM-rate parameters  $k_1, k_{-1}, k_2$ . This means that both models describe the process dynamics using

equivalent rate constants and, since we consider the HMM-system to be true, this implies that the approximate model is also valid under the assumption  $\varepsilon \ll 1$ . Our next numerical examples aim to examine what happens whenever the assumption  $\varepsilon \ll 1$  does not hold.

**Computational example 1.2.** Our second numerical example shows how the solutions start to deviate when  $s_0$  and  $e_0$  are close to each other (Figure 3). We can observe that with  $\varepsilon \sim 1$  the transient phase, related to the timescale  $t_c$ , takes much longer and the assumption that  $t_c \ll t_s$  is violated, thus invalidating the use of the MM-model. The goodness of the approximation of the complex  $c$  can be a better indicator of the applicability of the MM-model than the approximation of the substrate  $s$ , as  $c$  undergoes a boundary layer effect at the beginning of the reaction.

The values of the initial conditions used are as follows:  $s_0 = 100, e_0 = 50, c_0 = 0, p_0 = 0$ . As before, we use parameters (5) to calculate  $V_{max} = k_2 e_0, K_m = (k_{-1} + k_2)/k_1$ .

**Computational example 1.3.** In this numerical example  $\varepsilon > 1$ . The HMM-solution for the substrate is even closer to the exponential decay solution (Figure 4). As observed from the approximations of the complex in the same figure, with  $\varepsilon > 1$ , the MM-model is inapplicable due to the much longer timescale of the complex buildup.

The values of the initial conditions used for the given solution are as follows:  $s_0 = 100, e_0 = 400, c_0 = 0, p_0 = 0$ . Here and everywhere in the sequel  $V_{max} = k_2 e_0, K_m = (k_{-1} + k_2)/k_1$  using parameters (5).

The specific growth rate function  $\mu(s) = V_{max}s/(K_m + s)$  is visualized for reference (Figure 5).

**Case 2.  $K \gg 1$ .**

**Computational example 2.1.** In this numerical example  $\varepsilon \ll 1$  and the solutions of the three models (4), (2) and (11) are identical (Figure 6).

The values of the initial conditions used for the given solution are as follows:  $s_0 = 0.1, e_0 = 0.001, c_0 = 0, p_0 = 0$ .

**Computational example 2.2.** Although we have set the initial

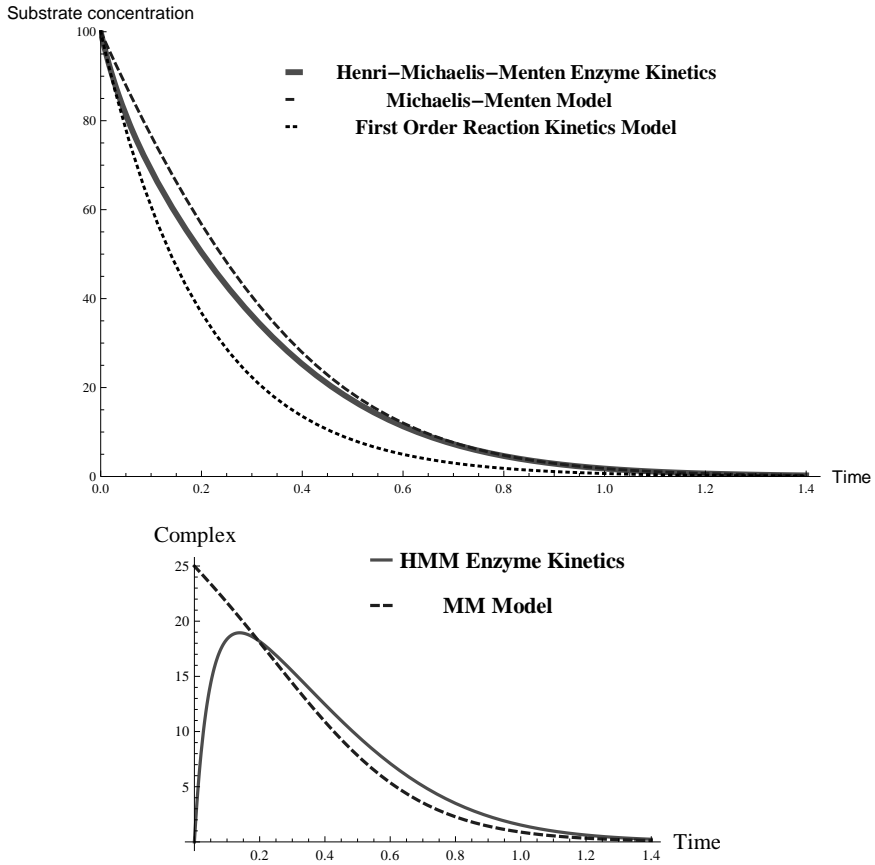


**Figure 3:** The solutions of the substrate (for models (2), (4), (11)) and the complex (for models (2), (4)) in the case  $\varepsilon = 0.5 \sim 1$ . Kinetic parameter values:  $k_1 = 0.1, k_{-1} = 0.01, k_2 = 10, K_m = (k_{-1} + k_2)/k_1 = 100.1, V_{max} = k_2 e_0 = 500$ ; initial conditions:  $s_0 = 100, e_0 = 50, c_0 = 0, p_0 = 0$ .

conditions so that  $\varepsilon \gg 1$ , the substrate solutions of the three models (4), (2) and (11) are still very close to each other (Figure 7).

The values of the initial conditions used in the models are as follows:  $s_0 = 0.1, e_0 = 2000, c_0 = 0, p_0 = 0$ .

The specific growth rate function  $\mu(s) = V_{max}s/(K_m + s)$  is visualized for reference (Figure 8).

As described above, in case 2:  $K \gg 1$  (also keeping in mind the

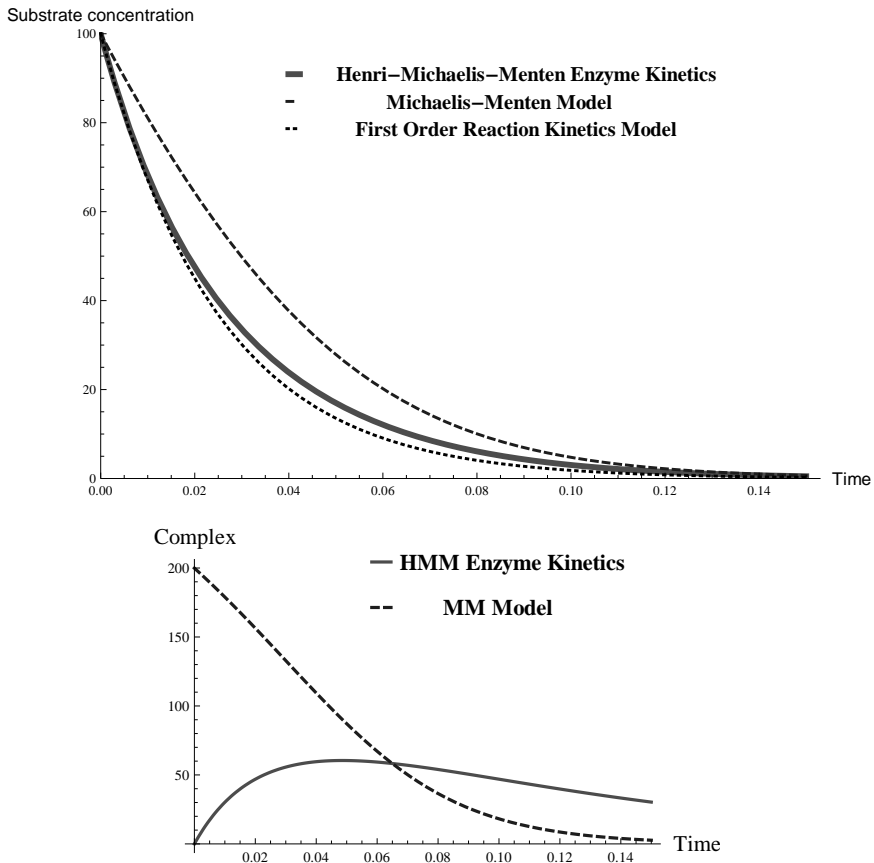


**Figure 4:** The solutions of the substrate (for models (4), (2), (11)) and the complex (for models (4), (2)) in the case  $\varepsilon = 4 > 1$ . Kinetic parameter values:  $k_1 = 0.1, k_{-1} = 0.01, k_2 = 10, K_m = (k_{-1} + k_2)/k_1 = 100.1, V_{max} = k_2 e_0 = 4000$ ; initial conditions:  $s_0 = 100, e_0 = 400, c_0 = 0, p_0 = 0$ .

assumption  $k_{-1} \ll k_2$ ), the MM-model can serve as a very good approximation to the Henri-Michaelis-Menten law in terms of substrate dynamics, regardless of the range of initial conditions. As seen from the solutions of the complex though (Figure 7), the MM-model completely fails to provide a good approximation of the complex dynamics when  $\varepsilon \gg 1$ . This is expected since the approximate model only provides the outer solutions of the system in the terms of singular pertur-

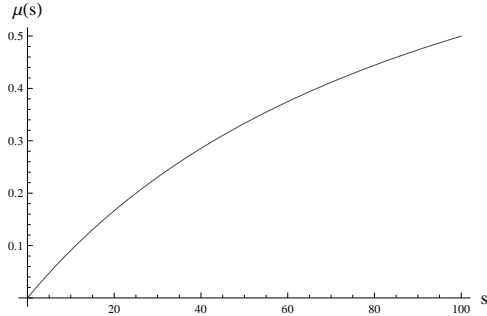


**Figure 5:** The specific growth rate function  $\mu(s) = V_{max}s/(K_m + s)$  from model (4) calculated in the range  $s$  from 0 to  $s_0 = 100$ . Case -  $\varepsilon = 10^{-3} \ll 1$ . Kinetic parameter values:  $k_1 = 0.1, k_{-1} = 0.01, k_2 = 10, K_m = (k_{-1} + k_2)/k_1 = 100.1, V_{max} = k_2e_0 = 1$ ; initial conditions:  $s_0 = 100, e_0 = 0.1, c_0 = 0, p_0 = 0$ .

bation analysis and in this case the inner solution has to be accounted for due to the longer timescale of the complex buildup process. According to the MM-model, the solution of the enzyme-substrate complex can be derived as  $c(t) = e_0s(t)/(K_m + s(t))$ , which under the proposed conditions ( $K \gg 1, k_{-1} \ll k_2$  and  $\varepsilon \gg 1$ ) cannot serve as a good approximation of the exact complex behavior. If we consider the non-dimensionalized system (9) under the same conditions, we can conclude that  $dv/d\tau \sim 0$  hence  $v = const$ .

The specific growth rate function (Figure 8) is almost linear in this case (again, regardless of whether  $\varepsilon \ll 1$  or  $\varepsilon \gg 1$ ) in contrast to case 1. It is thus natural to expect the approximate model to predict substrate solutions similar to exponential decay in this case.

Finally, the criterion (6) is obviously violated for computational example 2.2. (in contrast to all other examples where it is evaluated to less than 1):

$$\frac{k_2e_0}{k_1(s_0 + K_m)^2} = 19.9.$$

Nevertheless, since  $K \gg 1, k_{-1} \ll k_2$ , the proposed explanations in Section 3.1.1 are indeed manifested and the substrate solutions of all the three considered models are identical. As noted, this does not necessarily mean that the solutions of the other molecular species are correct, e.g. the MM-model solutions for the complex are incorrect in

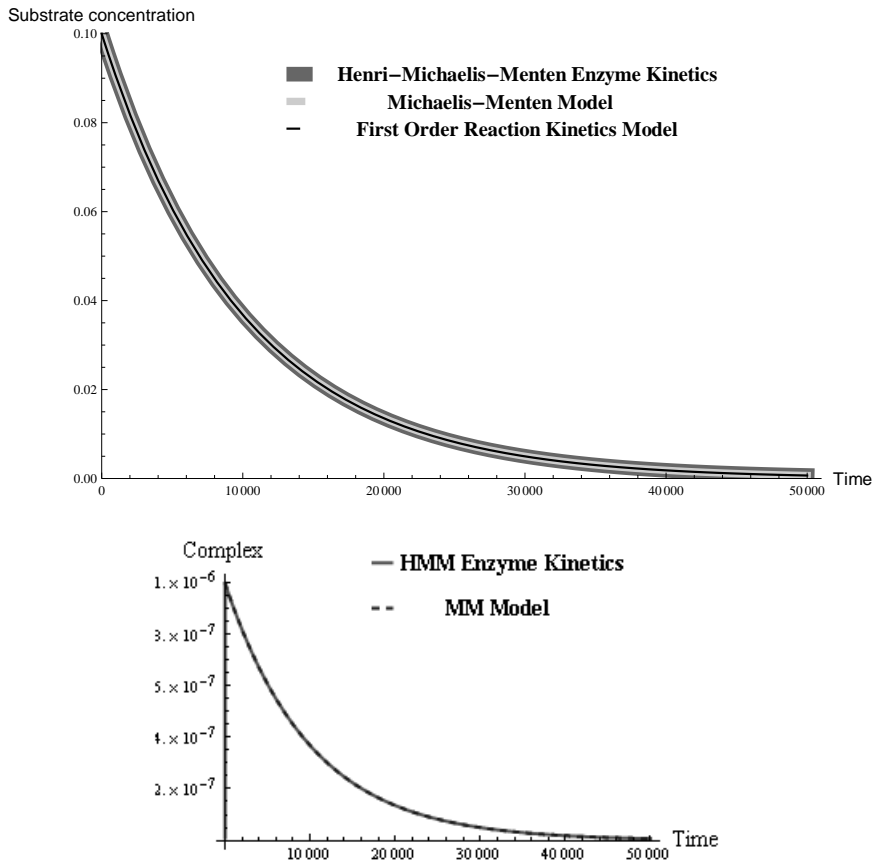


**Figure 6:** The solutions of the substrate (for models (4), (2), (11)) and the complex (for models (4), (2)) in the case  $\varepsilon = 0.01 \ll 1$ . Kinetic parameter values:  $k_1 = 0.1, k_{-1} = 0.01, k_2 = 10, K_m = (k_{-1} + k_2)/k_1 = 100.1, V_{max} = k_2 e_0 = 0.01$ ; initial conditions:  $s_0 = 0.1, e_0 = 0.001, c_0 = 0, p_0 = 0$ .

case  $\varepsilon \gg 1$ .

### 3.2 Summary

There exist theoretical cases when the decay model produces better approximation to the exact HMM-scheme than the MM-model. Additionally, in certain cases in which the MM-model can provide

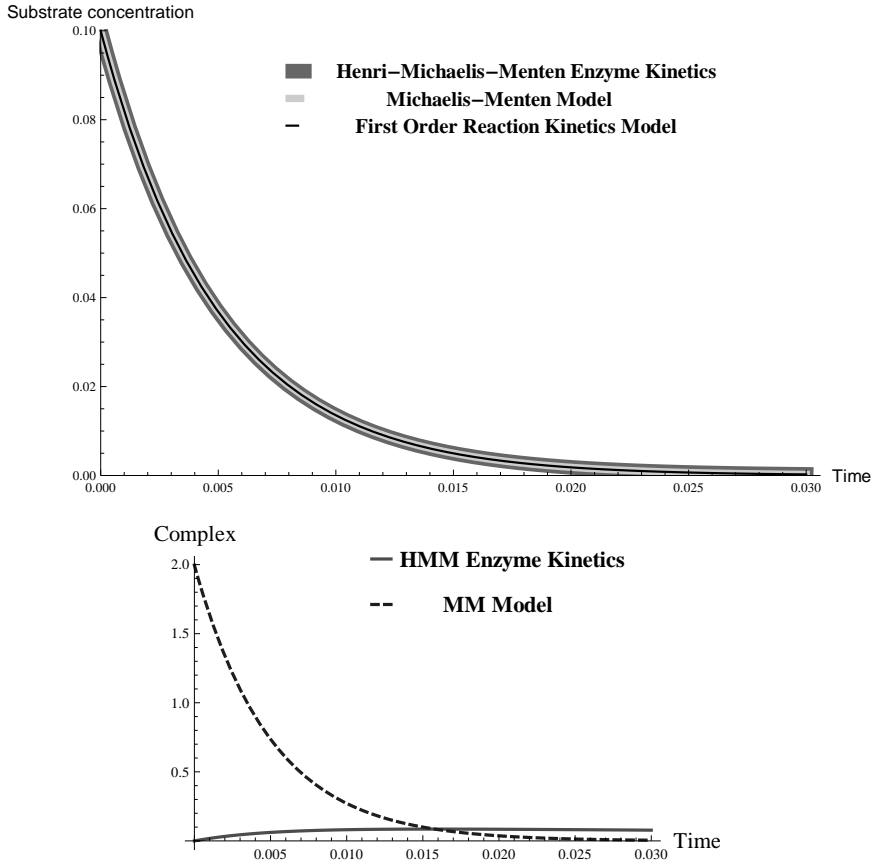


**Figure 7:** The solutions of the substrate (for models (4), (2), (11)) and the complex (for models (4), (2)) in the case  $\varepsilon = 2 * 10^4 \gg 1$ . Kinetic parameter values:  $k_1 = 0.1, k_{-1} = 0.01, k_2 = 10, K_m = (k_{-1} + k_2)/k_1 = 100.1, V_{max} = k_2 e_0 = 2 * 10^4$ ; initial conditions:  $s_0 = 0.1, e_0 = 2000, c_0 = 0, p_0 = 0$ .

good substrate approximations, it may completely fail to give correct estimates of the complex or enzyme behavior.

It has been demonstrated that the value of the Michaelis constant may strongly depend on the method of calculation. On the other hand, the rate constants in the enzyme kinetic Henri's reaction scheme are well-defined and can be efficiently computed from time course experimental data. Moreover, the modeling of metabolic pathways makes

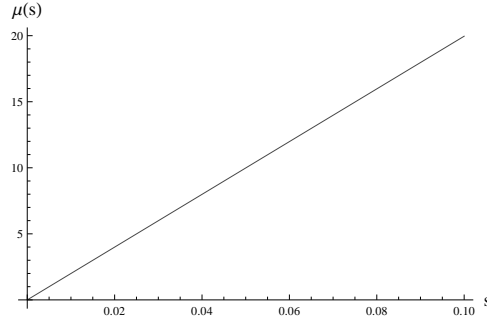


**Figure 8:** The specific growth rate function  $\mu(s) = V_{max}s/(K_m + s)$  from model (4) calculated in the range  $s$  from 0 to  $s_0 = 0.1$ . Case -  $\varepsilon = 2 * 10^4 \gg 1$ . Kinetic parameter values:  $k_1 = 0.1, k_{-1} = 0.01, k_2 = 10, K_m = (k_{-1} + k_2)/k_1 = 100.1, V_{max} = k_2e_0 = 2 * 10^4$ ; initial conditions:  $s_0 = 0.1, e_0 = 2000, c_0 = 0, p_0 = 0$ .

use of multiple reactions and can be made more rigorous when based on Henri's reactions instead of Michaelis-Menten approximate reactions, being especially imprecise when applied to living cells.

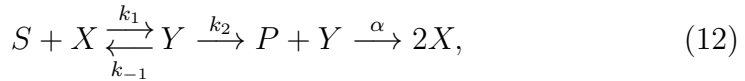
Such arguments confirm the need of refining the general methods for the determination of the Henri's reaction scheme rate constants. In addition the need of validation methods in combination with the availability of experimental data involving measurement errors [17] should be pointed out; a more detailed introduction of the use of validated interval methods is presented in [9].

Overall, the use of the Henri-Michaelis-Menten model allowed for the analysis essential for the explanation of the valid and invalid uses of the approximate Michaelis-Menten model. Furthermore, certain biological interpretations were only possible to draw based on that analysis.

## 4 Cell growth model with two cell fractions

Following from the conclusions in Section 3, we will next examine a reaction scheme modeling the process of cell growth. Previous works have dealt with the development of cell growth models based on reaction schemes [19], and in particular inspired by the Henri-Michaelis-Menten law. However, the proposed reaction scheme has not been comprehensively studied previously.

Let us examine the following reaction scheme:



where

$S$  denotes the substrate

$X$  denotes the inactive Lag-phase cells that do not divide

$Y$  denotes the active Log-phase cells that do divide

$P$  denotes the buildup of metabolic byproducts in the process of cell growth and development that lead up to the catalysis of cell division

$Q$  denotes the byproducts not used for the process of cell division

$k_1$  denotes the rate of growth of cells  $X$  as a result of the consumption of substrate  $S$

$k_{-1}$  denotes the backward rate of inactivation of cells  $Y$  back into cells  $X$

$k_2$  denotes rate of build up of metabolic byproducts essential for the cell division

$\alpha$  denotes the rate of increase of the cell ( $X$ ) population due to reproduction

$\beta$  denotes the rate of utilization of byproducts  $P$  for any other means, as well as their natural degradation

Using the law of mass action we derive the following model. We intentionally leave the equation for  $q$  out of the system as our interest is in the analysis of the dynamical behavior of  $s, x, y, p$  and they do not directly depend on the byproducts  $q$ .

$$\begin{aligned}
 ds/dt &= -k_1sx + k_{-1}y, \\
 dx/dt &= -k_1sx + k_{-1}y + 2\alpha py, \\
 dy/dt &= k_1sx - k_{-1}y - (\alpha + \beta)py, \\
 dp/dt &= k_2y - (\alpha + \beta)py,
 \end{aligned}
 \tag{14}$$

If  $[ ]$  denotes concentration then  $s = [S]$ ,  $x = [X]$ ,  $y = [Y]$ ,  $p = [P]$ . The system is closed with initial conditions:

$$s(0) = s_0, x(0) = x_0, y(0) = 0, p(0) = 0, \tag{15}$$

where  $s_0 > 0$ ,  $x_0 > 0$ . Additionally, due to biological considerations we will assume:

$$\begin{aligned}
 k_1 > 0, & \quad k_{-1} > 0, & \quad k_2 > 0, \\
 \alpha > 0, & \quad \beta > 0, & \quad s_0 > x_0,
 \end{aligned}
 \tag{16}$$

$$\alpha + \beta > k_2 \sim k_1 \gg k_{-1}, \tag{17}$$

$$\alpha > \beta. \tag{18}$$

Condition (17) follows from the common cell division timescales for eukaryotic cells [7], which suggest that mitosis is the fastest phase,

while previous phases of cell growth and buildup of metabolic products are slower. In our model the reactions  $S + X \xrightleftharpoons[k_{-1}]{k_1} Y$  are roughly equivalent to phase G1 of the cell cycle, reaction  $Y \xrightarrow{k_2} P + Y$  is roughly equivalent to phases S and G2 [7].

Condition (18) is set because we want to examine the system when cell division is dominating, rather than depletion of the metabolic byproducts that catalyze cell division and the resulting cell decay. The analysis of the model under condition  $\alpha \leq \beta$  is left for future work.

In order to study the system numerically and theoretically, we will make use of approximations with a solid biological motivation. They simplify the further analysis greatly and allow the use of techniques of numerical and graphical analysis of two-dimensional systems.

In all following numerical experiments system (14) and its approximations are considered dimensionless for simplicity. Units of time and concentration are thus intentionally omitted from all figures.

## 4.1 Case 1: Phase with no active cell division

### 4.1.1 Motivation

Starting from the initial stage when all cells are inactive, they need to undergo a cascade of phases in the cell cycle in order to become viable for cell division. As we assume that all cells are evenly distributed in space, with equal chance of interacting with substrate we could argue that there exists an initial phase when no cell division takes place. Instead, cells are in the process of growth which corresponds to the first reaction in reaction scheme (12). In the initial phase there is very limited cell division taking place, instead cells grow in size and build up essential byproducts that catalyze the cell division.

In the first stage of analysis we will focus on the initial phase, when cells do not divide, hence  $x + y = \text{const.}$

### 4.1.2 Deriving the model

Let us examine the condition  $x + y = c, c = \text{const}$ . Evaluating it at  $t = 0$ , taking the initial conditions into consideration, we obtain  $c = x_0$ . Additionally, it holds that  $x' + y' = 0$ . Summing up the second and the third equations in system (14) results in:

$$-k_1sx + k_{-1}y + 2\alpha py + k_1sx - k_{-1}y - (\alpha + \beta)py = 0,$$

$$(\alpha - \beta)py = 0.$$

For the purpose of this work, we will assume  $\alpha > \beta$ , meaning cell growth is the main reaction of interest and it dominates the dynamics of the interactions between  $y$  and  $p$ . The alternative would instead lead to cell death as if  $p$  had a toxic effect on the cells. This case will be left for future analysis.

#### Case $y = 0$

From  $x + y = x_0$  it follows that  $x = x_0 = \text{const}$ . Additionally,  $p' = 0$  and  $p(0) = 0$  thus  $p = 0$ . This leaves a single equation for  $s$ :  $s' = -k_1x_0s$ , which has an exponential decay as a solution. This case has no relevant biological interpretation.

#### Case $p = 0$

System (14) can be rewritten substituting  $y$  with  $y = x_0 - x$  and having  $p = 0$  as follows:

$$\begin{aligned} ds/dt &= -k_1sx + k_{-1}(x_0 - x), \\ dx/dt &= -k_1sx + k_{-1}(x_0 - x). \end{aligned} \tag{19}$$

Clearly  $s' = x'$ , thus using the initial conditions ( $x(0) = x_0, s(0) = s_0$ ) to find the integration constants, we can derive:

$$\begin{aligned}s &= x + s_0 - x_0, \\ s(0) &= s_0.\end{aligned}$$

As the solution for  $s$  can be found if the solution for  $x$  is known, we are left with a single differential equation:

$$\frac{dx}{dt} = -k_1x(x + s_0 - x_0) + k_{-1}(x_0 - x), \quad (20)$$

where

$$x(0) = x_0.$$

### 4.1.3 Equilibria and stability

First, we need to find the equilibrium points by solving the following algebraic equation:

$$-k_1(x + s_0 - x_0)x + k_{-1}(x_0 - x) = 0,$$

$$-k_1x^2 - (k_{-1} + k_1s_0 - k_1x_0)x + k_{-1}x_0 = 0.$$

The solutions are:

$$\begin{aligned}\hat{x}_1 &= \frac{-k_{-1} - k_1s_0 + k_1x_0 - \sqrt{4k_{-1}k_1x_0 + (-k_{-1} - k_1s_0 + k_1x_0)^2}}{2k_1}, \\ \hat{x}_2 &= \frac{-k_{-1} - k_1s_0 + k_1x_0 + \sqrt{4k_{-1}k_1x_0 + (-k_{-1} - k_1s_0 + k_1x_0)^2}}{2k_1}.\end{aligned}$$

The stability of the two points  $\hat{x}_1$ ,  $\hat{x}_2$  will be examined using linearization technique.

Let  $dx/dt = f(x)$ . We will find the closest linear approximation of ODE (20) near the equilibrium points  $\hat{x}_1$ ,  $\hat{x}_2$ . Close to an equilibrium point  $x^*$  ( $f(x^*) = 0$ ),  $f(x)$  could be approximated by:

$$f(x) \sim f(x^*) + f'(x^*)(x - x^*) = f'(x^*)(x - x^*)$$

If we denote  $y = x - x^*$ , then from  $dy/dt = dx/dt$  it follows:

$$\frac{dy}{dt} \sim f'(x^*)y,$$

the solution of which is  $y(t) \sim e^{f'(x^*)t}y(0)$ . Obviously if  $f'(x^*) < 0$ , then  $\lim_{t \rightarrow \infty} y(t) = 0$  and  $\lim_{t \rightarrow \infty} x(t) = x^*$ . If on the other hand,  $f'(x^*) > 0$ , then  $\lim_{t \rightarrow \infty} y(t) = \infty$  and  $\lim_{t \rightarrow \inf} x(t) = \infty$

Then the equilibrium point  $x^*$  is stable if  $f'(x^*) < 0$ , and it is unstable if  $f'(x^*) > 0$ .

$$f'(x) = -2k_1x - k_{-1} - k_1s_0 + k_1x_0,$$

For the two equilibrium points we can obtain:

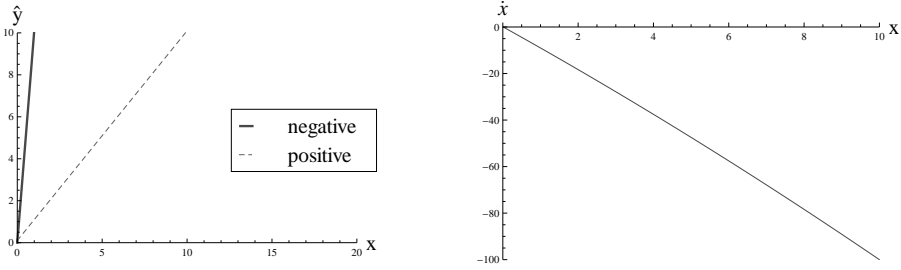
$$f'(\hat{x}_1) = \sqrt{4k_{-1}k_1x_0 + (k_1x_0 - k_{-1} - k_1s_0)^2},$$

$$f'(\hat{x}_2) = -\sqrt{4k_{-1}k_1x_0 + (k_1x_0 - k_{-1} - k_1s_0)^2}.$$

From  $k_{-1} > 0$ ,  $k_1 > 0$ ,  $x_0 > 0$  it follows that  $4k_{-1}k_1x_0 + (k_1x_0 - k_{-1} - k_1s_0)^2 > 0$  thus  $\hat{x}_1$  is unstable and  $\hat{x}_2$  is stable.

#### 4.1.4 Numerical experiments (no active cell division)

A rate balance plot indicates that the negative terms of equation (20) are larger in absolute value than the positive terms for  $x \in [0, x_0]$  and the used parameter values (Figure 9a). Thus, the solution for  $x$  in the considered cell growth phase is decreasing from the initial value of  $x_0$ . This is further supported by the plot of  $x$  against  $dx/dt$ , denoted  $\dot{x}$  (Figure 9b).



(a) A rate balance plot of equation (20). The line denoted negative is calculated via  $\hat{y} = x(k_{-1} + k_1 s_0 + k_1 x)$  for  $x \in [0, x_0]$ ; the line denoted positive is calculated via  $\hat{y} = k_{-1} x_0 + k_1 x x_0$  for the same interval for  $x$ . (b) The derivative of  $x$  is negative for  $x \in [0, x_0]$ ,  $x_0 = 10$ .

**Figure 9:** Analysis of equation (20). The parameter values and initial conditions for both plots are:  $x_0 = 10$ ,  $s_0 = 100$ ,  $k_{-1} = 0.01$ ,  $k_1 = 0.1$ .

Finally, the numerical solutions of equation (20) have been plotted (Figure 10). A relatively small change in the concentration of the substrate  $s$  can be observed. The activation of cells is illustrated by the decrease of inactive cells  $x$  and the corresponding increase in active cells  $y$ .

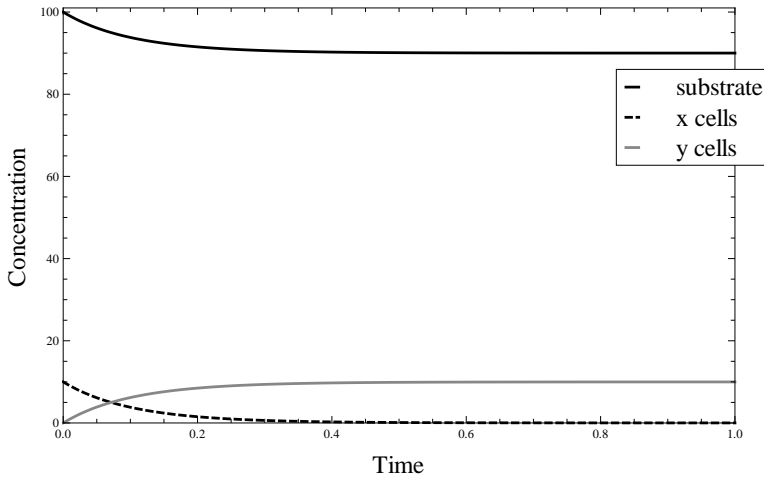


**Figure 10:** The numerical solutions of equation (20). Parameters values:  $k_{-1} = 0.01$ ,  $k_1 = 0.1$ ; initial conditions:  $x_0 = 10$ ,  $s_0 = 100$ .

## 4.2 Case 2: Active cell division phase

### 4.2.1 Motivation

Starting from the initial system (14) and taking another condition into consideration would in turn allow us to derive a more manageable system of ODEs for the phase of active cell division.

Let us first examine the points where  $p' = 0$ . From system (14) it follows that if  $p' = 0$ :

$$k_2y - (\alpha + \beta)py = 0,$$

$$(k_2 - (\alpha + \beta)p)y = 0.$$

Then either  $y = 0$  or  $p = k_2/(\alpha + \beta)$ . We will exclude the equation for  $p$  from the system, assuming that it has reached its steady state of  $p = k_2/(\alpha + \beta)$ . This is a reasonable assumption given that reactions  $P + Y \xrightarrow{\alpha} 2X$  and  $P + Y \xrightarrow{\beta} Q$  are much faster than  $Y \xrightarrow{k_2} P + Y$ , as the final phase in cell division usually has a much shorter time-scale than the phases of cell growth and buildup of metabolic products [7].

If the solution for  $p$  is monotonically increasing, that would mean the maximum value it would reach is much smaller under the aforementioned conditions (namely if the reaction of buildup of  $p$  is much slower than the reaction of uptake of  $p$ ).

We argue that the solution for  $p$  is a monotonically increasing function. Indeed, in the beginning of the reaction when both  $y$  and  $p$  are very small (note the initial conditions are  $p(0) = 0$ ,  $y(0) = 0$ ),  $p \ll 1$ ,  $y \ll 1$ . It is reasonable to assume  $(\alpha + \beta)py \ll k_2y$ . Thus,  $p$  increases initially until either  $y = 0$  or  $p = k_2/(\alpha + \beta)$ . It will be later proved that  $y = 0$  corresponds to a steady state of the approximate model. Additionally, numerical experiments show that solutions for  $y$  initially increase significantly, allowing  $p$  to reach its maximum value.

### 4.2.2 Deriving the model

Under the assumption that  $p$  has reached the value of  $k_2/(\alpha + \beta)$ , ODE system (14) can be rewritten as system (21):

$$\begin{aligned} ds/dt &= -k_1sx + k_{-1}y, \\ dx/dt &= -k_1sx + k_{-1}y + \gamma k_2y, \\ dy/dt &= k_1sx - k_{-1}y - k_2y, \end{aligned} \tag{21}$$

where

$$s(0) = s_1 > 0, x(0) = x_1 > 0, y(0) = y_1 > 0,$$

and

$$\gamma = \frac{2\alpha}{\alpha + \beta}.$$

We are only interested in the case  $\alpha > \beta$ , thus in the analysis in all following sections we will assume  $1 < \gamma \leq 2$ .

Let us now examine the sum of  $x' + y'$  and the difference  $x' - s'$ :

$$x' + y' = (\gamma - 1)k_2y,$$

$$x' - s' = \gamma k_2y.$$

Now,  $k_2y$  can be expressed in terms of  $x'$ ,  $s'$  and  $\gamma$  and substituted in the equation for  $x' + y'$  as follows:

$$\frac{x' - s'}{\gamma} = k_2 y,$$

$$x' + y' = (\gamma - 1) \frac{x' - s'}{\gamma},$$

$$x' = -\gamma y' - s'(\gamma - 1).$$

Integrating the above and using the initial conditions for the active cell growth phase we can derive:

$$\begin{aligned} x + c_1 &= -\gamma y - \gamma c_2 - (\gamma - 1)s - (\gamma - 1)c_3, \\ -c_1 - \gamma c_2 - (\gamma - 1)c_3 &= x_1 + \gamma y_1 + (\gamma - 1)s_1, \end{aligned}$$

$$x = x_1 + \gamma y_1 + (\gamma - 1)s_1 - \gamma y - (\gamma - 1)s,$$

where  $x_1, y_1, s_1$  are the values of  $x, y, s$  at the start of the phase, the initial conditions for system (21).

Finally for  $x(t)$  we have:

$$\begin{aligned} x(t) &= x_1 + \gamma y_1 + (\gamma - 1)s_1 - \gamma y(t) - (\gamma - 1)s(t), t > 0, \\ x(0) &= x_1. \end{aligned} \quad (22)$$

A substitution of the derived equation for  $x$  in system (21) results in the following system of two ODEs:

$$ds/dt = -k_1(x_1 + \gamma y_1 + (\gamma - 1)s_1 - \gamma y - (\gamma - 1)s)s + k_{-1}y, \quad (23)$$

$$dy/dt = k_1(x_1 + \gamma y_1 + (\gamma - 1)s_1 - \gamma y - (\gamma - 1)s)s + k_{-1}y - k_2y,$$

with initial conditions

$$s(0) = s_1, y(0) = y_1.$$

### 4.2.3 Equilibria and stability

The following algebraic system needs to be solved in order to find the equilibrium points of the system of ODEs (23):

$$\begin{aligned} -k_1(x_1 + \gamma y_1 + (\gamma - 1)s_1 - \gamma y - (\gamma - 1)s)s + k_{-1}y &= 0, \\ k_1(x_1 + \gamma y_1 + (\gamma - 1)s_1 - \gamma y - (\gamma - 1)s)s - k_{-1}y - k_2y &= 0. \end{aligned}$$

Summing up both equations we obtain:

$$-k_2y = 0.$$

From conditions (16) it follows that  $k_2 > 0$  and thus  $y = 0$ . Substituting  $y = 0$  into the first equation of the algebraic system we derive:

$$-k_1(x_1 + \gamma y_1 + (\gamma - 1)s_1 - (\gamma - 1)s)s = 0.$$

The two solutions of that equation are  $\{s_1 = 0, s_2 = (s_1(\gamma - 1) + \gamma y_1 + x_1)/(\gamma - 1)\}$ .

Finally, as  $y = 0$  the two equilibrium points are:

$$\begin{aligned} E_1 &= (0, 0), \\ E_2 &= \left( \frac{s_1(\gamma - 1) + \gamma y_1 + x_1}{\gamma - 1}, 0 \right). \end{aligned}$$

An observation about  $E_2$  is that the value for the substrate  $s$  is bigger than the initial condition  $s_1$  (note that  $\gamma > 1$ ):

$$\frac{s_1(\gamma - 1) + \gamma y_1 + x_1}{\gamma - 1} = s_1 + \frac{\gamma y_1 + x_1}{\gamma - 1} > s_1.$$

To study the local stability of the two equilibrium points we need to derive the Jacobi matrix of system (23):

$$J = \begin{pmatrix} \frac{\partial f_1}{\partial s} & \frac{\partial f_1}{\partial y} \\ \frac{\partial f_2}{\partial s} & \frac{\partial f_2}{\partial y} \end{pmatrix},$$

where  $f_1$  denotes the right-hand side of  $ds/dt$  in system (23), while  $f_2$  denotes the right-hand side of  $dy/dt$  in system (23).

Finally, it is easy to obtain:

$$J = \begin{pmatrix} -k_1(x_1 + \gamma y_1 + (\gamma - 1)s_1 - \gamma y - 2(\gamma - 1)s) & k_{-1} + k_1\gamma s \\ k_1(x_1 + \gamma y_1 + (\gamma - 1)s_1 - \gamma y - 2(\gamma - 1)s) & -k_{-1} - k_2 - k_1\gamma s \end{pmatrix}$$

### Local stability of Equilibrium point $E_1$ - ( $s = 0$ , $y = 0$ ).

The Jacobi matrix  $J$  evaluated at  $E_1$  is:

$$J(E_1) = \begin{pmatrix} -k_1(x_1 + \gamma y_1 + (\gamma - 1)s_1) & k_{-1} \\ k_1(x_1 + \gamma y_1 + (\gamma - 1)s_1) & -k_{-1} - k_2 \end{pmatrix}.$$

The eigenvalues of  $J(E_1)$  need to be found in order to study the local stability of equilibrium point  $E_1$ . If non-zero, their signs would determine whether the point is stable or unstable. Recall that the eigenvalues of a matrix  $A$  can be found by solving  $\det(A - \lambda E) = 0$ , where  $E$  is the identity matrix of the appropriate size. In our case that would be the identity matrix of size 2 because  $J(E_1)$  is a  $2 \times 2$  matrix.

Solving the resultant equation of  $\det(J(E_1) - \lambda E) = 0$ , the eigenvalues of  $J(E_1)$  are found to be:

$$\lambda_1 = -\frac{1}{2}(k_{-1} + k_2 + k_1(s_1(\gamma - 1) + x_1 + \gamma y_1) + \sqrt{(k_{-1} + k_2 + k_1(x_1 + s_1(\gamma - 1) + \gamma y_1))^2 - 4k_1k_2(x_1 + s_1(\gamma - 1) + \gamma y_1)},$$

and

$$\lambda_2 = -\frac{1}{2}(k_{-1} + k_2 + k_1(s_1(\gamma - 1) + x_1 + \gamma y_1) - \sqrt{(k_{-1} + k_2 + k_1(x_1 + s_1(\gamma - 1) + \gamma y_1))^2 - 4k_1k_2(x_1 + s_1(\gamma - 1) + \gamma y_1)}).$$

Let us denote  $\sigma = k_1(x_1 + s_1(\gamma - 1) + \gamma y_1)$  to simplify the analysis. It is first important to show that the eigenvalues are real ( $\lambda_1, \lambda_2 \in \mathbb{R}$ ). The following holds under rate conditions (16):

$$-4k_2\sigma + (k_{-1} + k_2 + \sigma)^2 > 0.$$

The validity of the inequality is obvious if the above is rewritten as:

$$-4k_2\sigma + (k_{-1} + k_2 + \sigma)^2 = k_{-1}^2 + (k_2 - \sigma)^2 + 2k_{-1}(k_2 + \sigma) > 0,$$

If we then compare the considered square root term with  $k_{-1} + k_2 + \sigma$ , taking their second power, we can obtain:

$$(k_{-1} + k_2 + \sigma)^2 > -4k_2\sigma + (k_{-1} + k_2 + \sigma)^2.$$

It then follows directly that under conditions (16), and more specifically if  $\sigma > 0$ ,  $k_1 > 0$ ,  $k_{-1} > 0$ ,  $k_2 > 0$ , both eigenvalues  $\lambda_1, \lambda_2$  are strictly negative and thus, the point  $E_1$  is a stable node.

**Local stability of Equilibrium point  $E_2$  - ( $s = (s_1(\gamma - 1) + \gamma y_1 + x_1)/(\gamma - 1)$ ,  $y = 0$ )**

The Jacobi matrix  $J$  evaluated at  $E_2$  is:

$$J(E_2) = \begin{pmatrix} k_1(x_1 + \gamma y_1 + (\gamma - 1)s_1) & k_{-1} + k_1\gamma \frac{s_1(\gamma-1) + \gamma y_1 + x_1}{\gamma-1} \\ -k_1(x_1 + \gamma y_1 + (\gamma - 1)s_1) & -k_{-1} - k_2 - k_1\gamma \frac{s_1(\gamma-1) + \gamma y_1 + x_1}{\gamma-1} \end{pmatrix}.$$

Denote  $\sigma = k_1(x_1 + s_1(\gamma - 1) + \gamma y_1) > 0$ . Matrix  $J(E_2)$  can then be rewritten as:

$$J(E_2) = \begin{pmatrix} \sigma & k_{-1} + \gamma \frac{\sigma}{\gamma-1} \\ -\sigma & -k_{-1} - k_2 - \gamma \frac{\sigma}{\gamma-1} \end{pmatrix}.$$

The eigenvalues of  $J(E_2)$  are:

$$\lambda_1 = -\frac{\left( (k_{-1} + k_2)(\gamma - 1) + \sigma \right) + \sqrt{4k_2(\gamma - 1)^2\sigma + \left( (k_{-1} + k_2)(\gamma - 1) + \sigma \right)^2}}{2(\gamma - 1)},$$

and

$$\lambda_2 = -\frac{\left( (k_{-1} + k_2)(\gamma - 1) + \sigma \right) - \sqrt{4k_2(\gamma - 1)^2\sigma + \left( (k_{-1} + k_2)(\gamma - 1) + \sigma \right)^2}}{2(\gamma - 1)}.$$

All parameters and initial conditions are strictly positive ( $k_{-1} > 0, k_1 > 0, k_2 > 0, x_1 > 0, s_1 > 0$ ), following from conditions (16), also  $\gamma > 1$  (condition (18)). Thus, the radicand in  $\lambda_1, \lambda_2$  is positive and it is obvious that all terms in the equation for  $\lambda_1$  are negative, thus  $\lambda_1 < 0$ .

The sign of  $\lambda_2$  depends on the sign of the nominator since  $\gamma > 1$  (condition (18)). Let us compare the squares of the positive term and the two negative terms of the nominator.

$$\left( (k_{-1} + k_2)(\gamma - 1) + \sigma \right)^2 < 4k_2(\gamma - 1)^2\sigma + \left( (k_{-1} + k_2)(\gamma - 1) + \sigma \right)^2$$

The positive term in the equation for  $\lambda_2$  is bigger than the negative term, hence  $\lambda_2 > 0$  and finally  $E_2$  is an unstable point (a saddle, due to the different signs of the eigenvalues).

An expected result would be to see the trajectories of the dynamical system approaching asymptotically the eigenvector associated with the positive eigenvalue. Numerical experiments confirm that behavior (Figure 12d) (note that  $E_2$  is visualized by the gray point on the axis  $y = 0$ ), the trajectories close to  $E_2$  are attracted by the point on the  $y$  axis and they are repelled by it on the  $s$  axis.

**Finding an estimate of the concentration of inactive cells ( $x$ ) when the system has reached equilibrium point  $E_1$**

The solution for  $x(t)$  obtained in Section 4.2.2, equation (22), and evaluated at  $t = t^*$ , where  $t^*$  corresponds to  $E_1$  is:

$$x(t^*) = x_1 + \gamma y_1 + (\gamma - 1)s_1. \quad (24)$$

From Section 4.1 we know that  $s = s_0 - x_0 + x$  for the case  $x + y = \text{const}$ . Under the assumption that the active cell division phase starts shortly after the phase where  $x + y = \text{const}$ , and the change in concentrations of substrate and cell populations is very small in-between the two phases, we can derive  $s_1$ , the initial substrate concentration at the beginning of the active division phase with:

$$s_1 = s_0 - x_0 + x_1.$$

Further, since  $x + y = \text{const} = x_0$  for the duration of the phase with no active cell division:

$$s_1 = s_0 - x_0 + x_1 = s_0 - x_0 + x_0 - y_1 = s_0 - y_1.$$

Substituting the above in equation (24) we obtain:

$$x(t^*) = x_1 + \gamma y_1 + (\gamma - 1)(s_0 - y_1),$$

$$x(t^*) = x_1 + y_1 + (\gamma - 1)s_0.$$

Again assuming the insignificant change in concentration of  $x, y, s$  between the two phases we finally have:

$$x(t^*) = x_0 + (\gamma - 1)s_0, \quad (25)$$

$$\gamma = \frac{2\alpha}{\alpha + \beta}. \quad (26)$$

The concentration of all living cells at  $E_1$  is equal to the concentration of inactive  $x$  cells since  $y = 0$ . Given that also  $1 < \gamma \leq 2$  we obtain  $x_0 < x(t^*) \leq x_0 + s_0$ .

#### 4.2.4 Numerical experiments (active cell division)

Having an insight about the dynamical system's behavior, as well as certain characteristics of the equilibrium points, is essential. The nullclines of system (23) are thus plotted on (Figure 11). There is only one point where the two lines intersect, that is at  $y = s = 0$ . As proved in Section 4.2.3 this is a stable node.

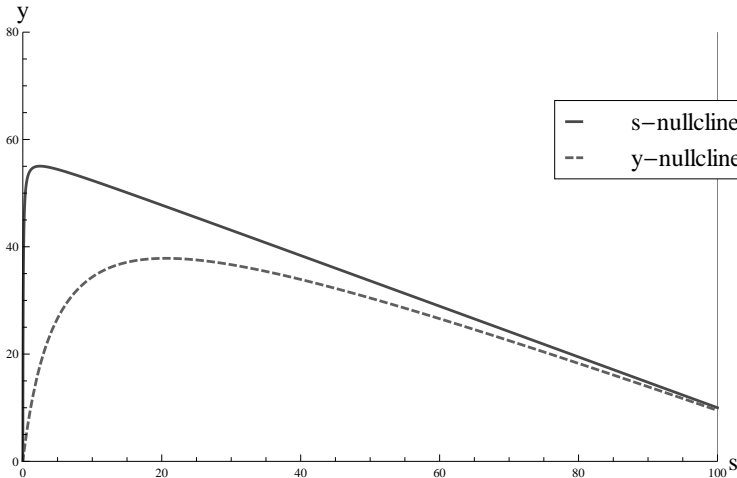


**Figure 11:** The nullclines of the system (23). Parameter values:  $k_{-1} = 0.01, k_1 = 0.1, k_2 = 1, \gamma = 1.9$ ; initial conditions:  $y_1 = 10, s_1 = 100$ .

It is clearly visible from the phase portrait of the system (Figure 12) that the expected behavior is for solution of the substrate to be monotonically decreasing, while solutions of the active cells are initially increasing to their maximum value and then decreasing to 0. If the condition  $x_0 \ll s_0$  holds, it can be argued that  $y_1 \ll s_1$ . Then solutions cross the  $y$ -nullcline exactly once and never cross the  $s$ -nullcline. If, however,  $y_1 \sim s_1$  solutions cross the  $y$ -nullcline two times thus the solution for  $y$  is first decreasing, then increasing and finally decreasing again until it reaches the value of 0 (Figure 12d).

For biologically reasonable relations (conditions (17), (18)) between the parameters of system (23), numerical experiments show that the solution for  $p$  reaches its maximum of  $k_2/(\alpha + \beta)$  (Figure 13).

Finally, system (21) has been solved numerically (Figure 14). Numerical

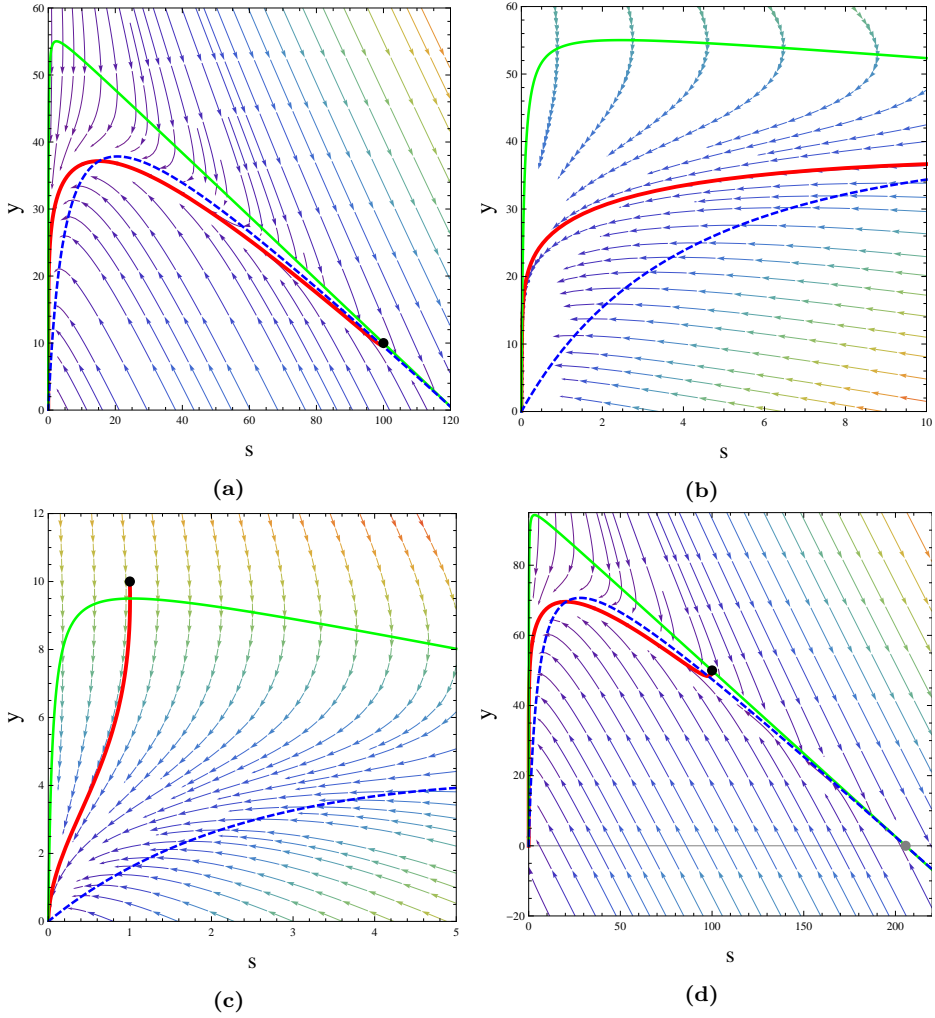


**Figure 12:** Phase portraits of system (23) showing the dynamics of a solution (red line) with initial conditions:  $y_1 = 10, s_1 = 100$  and parameter values:  $k_{-1} = 0.01, k_1 = 0.1, k_2 = 1, \gamma = 1.9$ . In all plots the green line is the  $s$ -nullcline, the blue line is the  $y$ -nullcline. (a) The phase portrait along with a solution of the system. (b) The behavior for  $s \in [0, 10]$  illustrating dynamics close to the steady state. (c) The phase portrait of the system when  $s_1 = 1$  and all other initial conditions and parameters being unchanged. (d) The phase portrait of the system when  $y_1 = 50, s_1 = 100$ , showing that the solution crosses the  $y$ -nullcline twice.

experiments confirm that under the considered conditions (17), (18) cells grow up to concentrations in the range  $(x_0, x_0 + s_0]$ , which depends on the

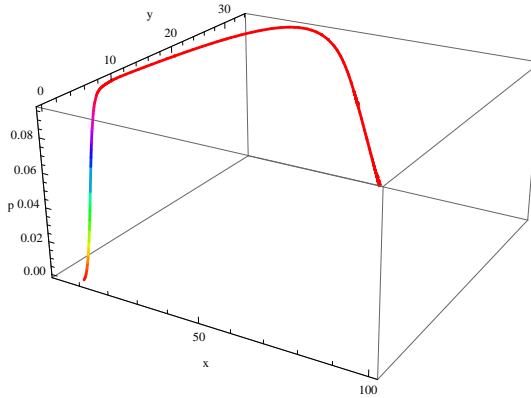


**Figure 13:** A parametric plot of the numerical solutions of system (14) as a function of  $x$ ,  $y$ ,  $p$ . Parameter values:  $k_{-1} = 0.01, k_1 = 0.1, k_2 = 1, \alpha = 10, \beta = 0.5$ ; initial conditions:  $y_1 = 10, s_1 = 100$ . The color of the solution signifies change in value of  $p$ .

rate constants  $\alpha$  and  $\beta$  as outlined in equation (25).

### 4.3 Numerical experiments

The initial system (14) was solved numerically for a set of initial conditions and parameter values:  $k_{-1} = 0.01, k_1 = 0.1, k_2 = 1, \alpha = 10, \beta = 0.5, x_0 = 10, s_0 = 100, y_0 = 0, p_0 = 0$ . As above, all parameters and initial conditions are considered dimensionless.

The experiments confirm the validity of the approximations made in Section 4.1 and Section 4.2. Indeed, initially there is very little or no cell growth observable (Figure 16). The values of the parameters and initial conditions are kept in line with conditions (17), (18).

Furthermore, under the aforementioned conditions the solution for  $p$  reaches its maximum before the active cell division phase takes place (Figure 16).

Although the case of rate constants  $\alpha$  and  $\beta$  being equal is not discussed in this work, a numerical experiment is presented to illustrate the behavior of the solutions (Figure 17). As we can see, there is no cell growth during the whole process, while the substrate is completely utilized.

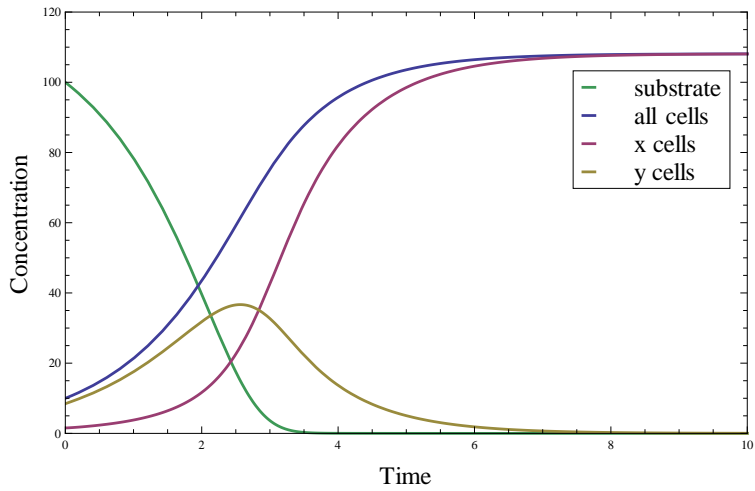


**Figure 14:** Numerical solutions of system (23). Parameter values:  $k_{-1} = 0.01, k_1 = 0.1, k_2 = 1, \alpha = 10, \beta = 0.5, \gamma \sim 1.9$ ; initial conditions:  $y_1 = 10, s_1 = 100$ .

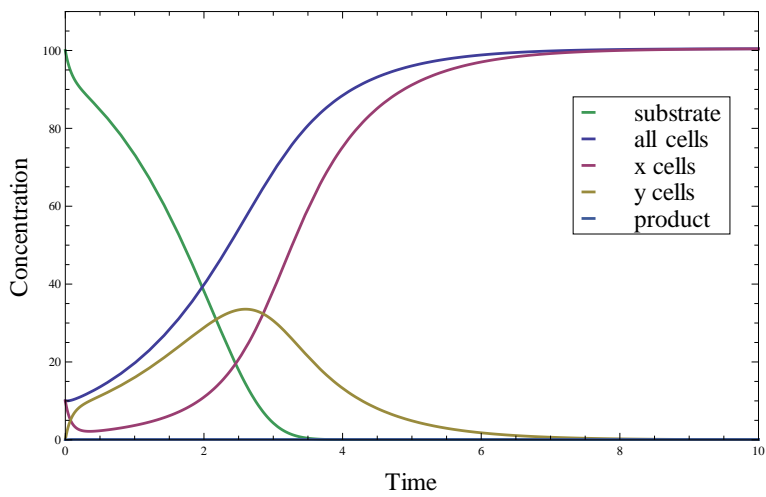
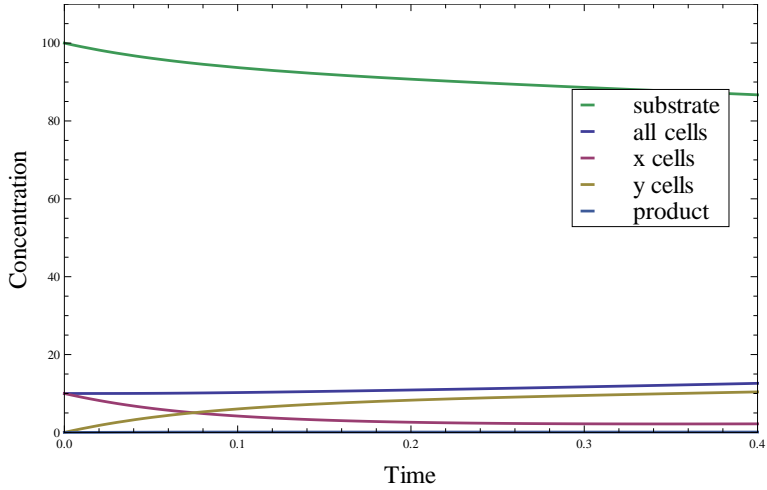
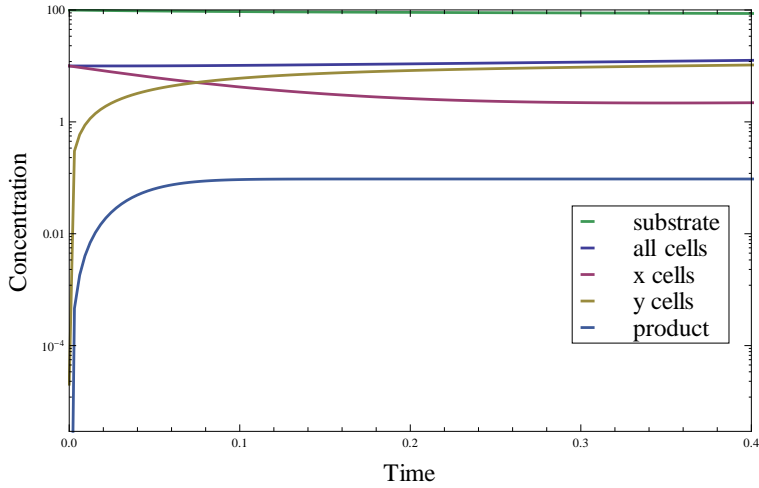


**Figure 15:** The numerical solutions of system (14). Parameter values:  $k_{-1} = 0.01, k_1 = 0.1, k_2 = 1, \alpha = 10, \beta = 0.5$ ; initial conditions:  $x_0 = 10, s_0 = 100$ .



(a) There is very little cell growth in this phase, rather there is product buildup to the point of its maximum value.



(b) A logarithmic scale plot showing the dynamics of the product along with the active and inactive cells.

**Figure 16:** The solutions of system (14) in the timescale when there is no cell growth. Parameter values:  $k_{-1} = 0.01$ ,  $k_1 = 0.1$ ,  $k_2 = 1$ ,  $\alpha = 10$ ,  $\beta = 0.5$ ; initial conditions:  $x_0 = 10$ ,  $s_0 = 100$ .

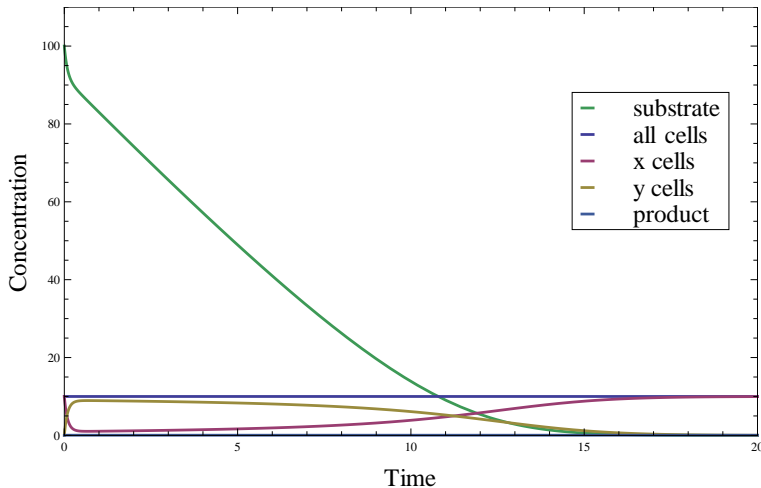


**Figure 17:** The numerical solutions of system (14) when  $\gamma \sim 1$  or  $\gamma = 1$ . Parameter values:  $k_{-1} = 0.01, k_1 = 0.1, k_2 = 1, \alpha = 10, \beta = 10$ ; initial conditions:  $x_0 = 10, s_0 = 100$ . There is no cell growth in this case, only activation and deactivation of the cells, while the substrate is being completely depleted in the process.

## 4.4 Summary

The derived dynamical system (14) along with the reaction scheme (12) it is based on, show promising results in modeling the process of cell growth. The behavior of the solution for  $s$  is of particular interest because it is difficult for phenomenological models of Monod type to replicate experimental results closely. Numerical experiments for system (14) show that there is a sharp decrease in substrate concentration during the initial phase, followed by a slower decay during the phase of active cell division (Figure 15).

The analysis of the approximate model for the active cell division phase (23) proves the existence of an unstable equilibrium and a stable equilibrium:

$$E_1 = (0, 0),$$

$$E_2 = \left( \frac{s_1(\gamma - 1) + \gamma y_1 + x_1}{\gamma - 1}, 0 \right),$$

where  $E_1$  is a stable node and  $E_2$  is unstable - a saddle point.

An interval has been found, under certain conditions, for the resulting concentration of inactive cells after the growth process has finished. This is valid under the conditions that  $p = k_2/(\alpha + \beta)$  at the beginning of the active cell division phase, as well as that there has been an insignificant change in concentration of  $s, x, y$  in-between the two considered phases (4.1) and (4.2). It then follows that  $x_0 < x(t^*) \leq x_0 + s_0$ , where  $t^*$  corresponds to the stable fixed point of the phase of active cell division.

## 5 Discussion

A central focus of this work is to prove the case for the use of mechanistic models induced by reaction schemes in the context of enzyme kinetics and cell growth. While the proposed model analyzed in Section 4 shows promising results for further analysis and validation against experimental data, it is important to discuss certain limitations that have been recognized.

A complete biological interpretation is yet to be given for the byproducts  $P$  of reaction scheme (12). The question about its intercellular and/or intracellular role in the process of cell division is central in the development of the model. Previous works have identified the necessity to introduce a micro scale and a macro scale for reactions modeling metabolic processes of living cells where intracellular interactions are considered as well as intercellular reactions [31].

The motivation for the approximate model (Section 4.2) is based on numerical experiments, as well as the physical nature of the process at hand. More solid theoretical evidence is required in order to unambiguously define the validity of that case. The employed methods of finding equilibria and assessing their stability are insufficient to study the original system of ODEs (14), hence more advance techniques are necessary.

In order to evaluate the significance and applicability of approximate model (23), it has to be compared to models focusing on the same cell growth phase. The Monod-type models are a good starting point for such an evaluation. It is of great interest to determine whether the simplified model that follows from a reaction scheme inspired by the Henri-Michaelis-Menten reaction scheme, would be able to perform as well as, or better than, a Monod-type model in the context of cell growth. Ease of use in

numerical experiments, goodness of fit against experimental data, ability to provide further insights about the biological process are only a few of the criteria for analysis. Results from such studies will determine future directions of development for the model.

It is true that certain models following from reaction schemes that describe cell growth processes can be cumbersome to analyze. They are usually non-linear, involve many variables, and are difficult to handle using simple but popular dynamical systems analysis techniques. With the analysis of the proposed model in Section 4 it has been proved that it is possible to analyze such models even with simple methods. Essential for the process is the understanding of the underlying physical phenomenon and the ability to recognize valid simplifications that greatly help reduce the complexity of the required work.

The software tools CAS Mathematica and MATLAB have been used in this work as computational tools, however, other suitable software tools can be used as well, such as COPASI [15], [20].

## 6 Conclusions

Classical enzyme kinetics models, such as the Henri-Michaelis-Menten model, the Michaelis-Menten model and the exponential decay model have been examined and compared in a numerical experiment. There exist cases when results of data fitting from approximate models can be very misleading about the dynamical behavior they suggest. Validation techniques and validity conditions are briefly reviewed.

A novel cell growth model has been proposed and studied analytically, making use of approximations with a solid biological motivation. They have further simplified the analysis and allowed the use of techniques, numerical and graphical analysis of two-dimensional systems.

Numerical experiments demonstrate the validity of the proposed approximations in biologically meaningful cases. They further help visualize the dynamical behavior of the system, shedding light on the plausibility of the studied model in the context of cell growth.

When modeling kinetic reactions or metabolic processes in living cells the suggested approach is to start with a description of the process by

biochemical reaction equations (schemes) and then pass to mathematical differential equations via the mass action principle. Such an approach is useful in keeping close to the biochemical mechanism of the modeling process; the use of this approach is recommended not only in fields like enzyme kinetic and metabolic networks but also in fields like cell growth and population dynamics [19].

## Acknowledgements

I would like to express my sincere gratitude to my supervisor Professor Svetoslav Markov for the continuous support and guidance throughout the writing of this thesis and related research. His immense knowledge, expertise and patience contributed considerably to my graduate experience.

I am grateful to Professor Tatyana Chernogorova, Professor Stefka Dimova, Assistant Professor Tihomir Ivanov and all other members of the Department of Numerical Methods and Algorithms for their help and support.

## References

- [1] K. R. Albe, M. H. Butler, B. E. Wright, Cellular concentrations of enzymes and their substrates, *J. Theor. Biol.* 143 (1990) 163–195.
- [2] M. N. Berberan-Santos, A general treatment of Henri-Michaelis-Menten enzyme kinetics: exact series solution and approximate analytical solutions, *MATCH Communications in Mathematical and in Computer Chemistry.* 63 (2010) 283–318.
- [3] A. M. Bersani, G. Dell’Acqua, Is there anything left to say on enzyme kinetic constants and QSSA?, *J. Math. Chem.* 50 (2012) 335–344.
- [4] A. M. Bersani, E. Bersani, G. Dell’Acqua, M. G. Pedersen, New trends and perspectives in nonlinear intracellular dynamics: one century from Michaelis-Menten paper, *Continuum Mech. Thermodyn.* 27 (2014) 659–684.
- [5] G. E. Briggs, J. B. S. Haldane, A note on the kinetic of enzyme action, *Biochem. J.* 19 (1925) 338–339.

- [6] W. W. Chen, M. Niepel, P. K. Sorger, Classic and contemporary approaches to modeling biochemical reactions, *Genes. Dev.* 24 (2010) 1861–1875.
- [7] Geoffrey M. Cooper, Robert E. Hausman. *The Cell: A Molecular Approach*. Washington, D.C.: ASM Press, 2009.
- [8] U. Deichmann, S. Schuster, J.-P. Mazat, A. Cornish-Bowden, Commemorating the 1913 Michaelis-Menten paper *Die Kinetik der Invertinwirkung: three perspectives*, *FEBS Journal.* 281 (2014) 435–463, in: J.-P. Mazat, Part 3:pp.452–463.
- [9] S. Dimitrov, G. Velikova, V. Beshkov, S. Markov, On the Numerical Computation of Enzyme Kinetic Parameters. *Biomath Communications* 1(2) (2014) <http://dx.doi.org/10.11145/j.bmc.2015.02.201>
- [10] S. Dimitrov, S. Markov, Metabolic rate constants: Some computational aspects, *Mathematics and Computers in Simulation.* 133 (2017), 91–110.
- [11] R. Grima, N. G. Walter, S. Schnell, Single molecule enzymology à la Michaelis-Menten, *FEBS J.* 281 (2014) 518–530.
- [12] S. M. Hanson, S. Schnell, The reactant stationary approximation in enzyme kinetics, *J. Phys. Chem. A* 112 (2008) 8654–8658.
- [13] V. Henri, Recherches sur la loi de l’action de la sucrase, *C. R. Hebd. Acad. Sci.* 133 (1901) 891–899.
- [14] V. Henri, *Lois générales de l’action des diastases*, Paris: Librairie Scientifique A. Hermann. 1903.
- [15] S. Hoops et al, COPASI—a complex pathway simulator, *Bioinformatics.* 22 (24) (2006) 3067–3074.
- [16] K. A. Johnson, R. S. Goody, The original Michaelis constant: translation of the 1913 Michaelis-Menten paper, *Biochemistry.* 50(39) (2011) 8264–8269.
- [17] W. Kraemer, J. Wolff v. Gudenberg (Eds), *Scientific Computing, Validated Numerics, Interval Methods*, Proc. of SCAN-2000/Interval-2000, Kluwer/Plenum, 2001.

- [18] K. J. Laidler, Theory of the transient phase in kinetics, with special reference to enzyme systems, *Can. J. Chem.* 33 (1955) 1614–1624.
- [19] S. Markov, Cell growth models using reaction schemes: batch cultivation, *Biomath.* 2(2) (2013) 1312301 1–9.
- [20] P. Mendes, S. Hoops, S. Sahle, R. Gauges, J. Dada, U. Kummer, Computational modeling of biochemical networks using COPASI, *Methods Mol. Biol.* 500 (2009) 17–59.
- [21] L. Michaelis, M. L. Menten, Die Kinetik der Invertinwirkung, *Biochem. Z.* 49 (1913) 333–369.
- [22] J. D. Murray, *Mathematical Biology: I. An Introduction*, third ed., Springer, 2002.
- [23] M. H. M. Olsson, P. E. M. Siegbahn, A. Warshel, Simulations of the large kinetic isotope effect and the temperature dependence of the hydrogen atom transfer in lipoxygenase, *J. Am. Chem. Soc.* 126 (9) (2004) 2820–2828.
- [24] M. G. Pedersen, A. M. Bersani, E. Bersani, The quasi steady-state approximation for fully competitive enzyme reactions, *Bull. Math. Biol.* 69 (2007) 433–457.
- [25] M. G. Pedersen, A. M. Bersani, E. Bersani, G. Cortese, The total quasi-steady-state approximation for complex enzyme reactions - A word of caution, *Math. Comput. Simul.* 79 (2008) 1010–1019.
- [26] S. Schnell, P. K. Maini, Enzyme kinetics at high enzyme concentration, *Bull. Math. Biol.* 62 (2000) 483–499.
- [27] S. Schnell, P. K. Maini, A century of enzyme kinetics: Reliability of the  $K_m$  and  $v_{max}$  estimates, *Comments Theor. Biol.* 8 (2003) 169–187.
- [28] S. Schnell, Validity of the Michaelis-Menten equation - Steady-state, or reactant stationary assumption: that is the question, *FEBS J.* 281 (2014) 464–472.
- [29] M. E. Stroppolo, M. Falconi, A. M. Caccuri, A. Desideri, Superefficient enzymes, *Cell. Mol. Life Sci.* 58 (2001) 1451–1460.

- [30] L. Stryer, J. M. Berg, J. L. Tymoczko, *Biochemistry*, fifth ed., New York: W H Freeman, 2002.
- [31] G. Velikova, T. Ivanov, *Mathematical Models Describing Biological Systems under Inhibitory Conditions*, Master Thesis, Sofia University “St. Kl. Ohridski”, 2015.
- [32] I. B. Wilson, M. A. Harrison, Turnover number of acetylcholinesterase, *J. Biol. Chem.* 236 (8) (1961) 2292–2295.